Sodium azide induces mitochondria-mediated apoptosis in PC12 cells through Pgc-1α-associated signaling pathway

YUANYI ZUO[1,2], JUN HU[1], XUEHUA XU[1], XIANGTING GAO[1], YUN WANG[1] and SHAOHUA ZHU[1]

[1]Department of Forensic Medicine, Medical College of Soochow University, Suzhou, Jiangsu 215123; [2]Department of Forensic Identification, Binhai People's Hospital, Yancheng, Jiangsu 224500, P.R. China

Received March 21, 2018; Accepted November 27, 2018

DOI: 10.3892/mmr.2019.9853

Abstract. Sodium azide (NaN_3), an inhibitor of cytochrome oxidase, induces the release of excitotoxins via an energy impairment and this, in turn, results in neurodegeneration. The present study aimed to investigate the toxic effects NaN_3 on apoptosis of PC12 cells and its mechanism of action in peroxisome proliferator-activated receptor γ co-activator 1-α (Pgc-1α)-associated signaling pathways. To induce apoptosis, PC12 cells were exposed to NaN_3 (0, 5, 10, 20, 40 and 80 mM) for 12, 24, 48 and 72 h. Cell viability was determined by CCK-8 assay. DAPI staining was employed to additionally examine apoptotic cells and their nuclear changes. Production of reactive oxygen species (ROS), mitochondrial membrane potential (ΔΨm) and apoptotic rate were also assessed by flow cytometry. Cellular ATP content was estimated by firefly luciferase assay. In addition, the expression levels of B-cell lymphoma 2 (Bcl-2), Bcl-2-associated X protein (Bax), phosphorylated (p)-Ca^{2+}/calmodulin-dependent protein kinase (CaMK), p-p38 mitogen-activated protein kinase (p38 MAPK), Pgc-1α, nuclear respiratory factor (Nrf)-1, mitochondrial transcription factor A (Tfam), p-extracellular signal-regulated kinase (Erk)1/2, Nrf-2 and complex IV (Cox IV) were determined by western blot analysis. The data suggested that NaN_3 may induce PC12 cell injury and dose-dependently decrease the cell viability. The expression levels of pro-apoptotic proteins Bax and cytochrome c were upregulated, while the expression levels of anti-apoptotic proteins procaspase-3 and Bcl-2 were downregulated. In addition, the phosphorylation of MAPK and Ca^{2+}/calmodulin-dependent protein kinase II (CaMKII) family members including pan-calcineurin A was increased, in particular the ratios of p-p38/p38 and p-CaMKII/CaMKII. However, the expression levels of Pgc-1α and its associated proteins, including Nrf-1/2, Tfam and p-Erk1/2 were decreased. In addition, mitochondria were the target organelles of NaN_3-induced toxicity in PC12 cells, which moderated the dissipation of ΔΨm, preserved the cellular ATP content, promoted the production of ROS and increased the apoptotic rate. These results suggested that NaN_3 induced cell death in PC12 cells via Pgc-1α-associated signaling pathways and provided a theoretical basis for additional investigation of the neurotoxic mechanism of NaN_3, with applications in neurodegenerative disorders.

Introduction

As a white, colorless and crystalline powder, sodium azide (NaN_3) is classed as a highly toxic substance. Its toxic effects are similar to those of cyanide, and it injures the nervous and cardiovascular systems, eyes and skin. This toxic element becomes active rapidly following ingestion, and its major effects occur several hours following oral intake, depending on the amount ingested (1,2). Exposure to NaN_3 may induce a number of symptoms within minutes, including nausea, vomiting, headache, restlessness, dizziness, weakness, rapid breathing and rapid heartbeat (3). High amounts of this toxic element immediately induce convulsions, loss of consciousness, low heart rate and blood pressure, and respiratory failure, eventually leading to mortality (3). Among the demonstrated action mechanisms of NaN_3, the most relevant one is cytochrome c oxidase-respiratory chain complex-inhibition (4). Previous studies have revealed that NaN_3, an inhibitor of complex IV (Cox IV), may induce apoptosis in primary cortical neurons, which is caspase-3 dependent and associated with the release of cytochrome c (5).

In mitochondrial biosynthesis, the promoter of respiratory chain Cox IV may be activated by nuclear respiratory factors (Nrf)-1/2. Concomitantly, Nrf may be adjusted by regulating

Correspondence to: Professor Shaohua Zhu, Department of Forensic Medicine, Medical College of Soochow University, 178 East Gan Jiang Road, Suzhou, Jiangsu 215123, P.R. China
E-mail: zhushaohua@suda.edu.cn

Abbreviations: NaN_3, sodium azide; Cox IV, complex IV; Tfam, mitochondrial transcription factor A; Nrf-1/2, nuclear respiratory factor-1/2; CaN, pan-calcineurin A; Pgc-1α, peroxisome proliferator-activated receptor γ co-activator 1-α; PC12, rat pheochromocytoma; ΔΨm, mitochondrial membrane potential; CCCP, carbonyl cyanide 3-chlorophenylhydrazone; ROS, reactive oxygen species; FCM, flow cytometry; MAPK, mitogen-activated protein kinase

Key words: sodium azide, PC12 cells, apoptosis, mitochondria, nuclear co-activator of peroxisome proliferator-activated receptor γ, toxicology

the activity of genes encoding mitochondrial transcription factor A (Tfam) to indirectly regulate the expression levels of respiratory chain genes. Nrf-1/2, Tfam, peroxisome proliferator-activated receptor γ co-activator 1-α (Pgc-1α) and other co-activators constitute the Pgc-1α signal cascade, which serves a central role in a regulatory network governing the transcriptional control of mitochondrial biogenesis and respiratory function. In this signal cascade, Pgc-1α first activates Nrf-1/2 as opposed to directly binding to the mitochondrial DNA, and Nrf-1/2 induces the activation of Tfam in combination with the promoter of Tfam and triggers the transcription and replication of mitochondrial DNA, leading to increased expression levels of mitochondrial proteins (6). Concurrently, Pgc-1α may be activated by CaN-, Ca^{2+}/calmodulin-dependent protein kinase (CaMK)-, mitogen-activated protein kinase (MAPK)- and cyclin-dependent kinase-mediated signaling pathways (7). In the present study, PC12 cells were used to generate a dopamine neuron model, and the effects and mechanism of NaN_3 on the Pgc-1α-associated pathways in PC12 cells were investigated, to identify whether NaN_3 induced toxicity in cultured PC12 cells and the underlying mechanisms involved in these effects.

Materials and methods

Materials. Rat pheochromocytoma PC12 cells were purchased from the Cell Bank of Type Culture Collection of the Chinese Academy of Sciences (Shanghai, China). Stock solution of NaN_3 (Sigma-Aldrich; Merck KGaA, Darmstadt, Germany) was dissolved in the sterile saline to make a 1 M stock solution, which was subsequently diluted to desired concentrations prior to experimentation. A one-step TUNEL Apoptosis Assay kit (C1090), Annexin V-fluorescein isothiocyanate (FITC) Apoptosis Detection kit (C1063), Enhanced adenosine 5'-triphosphate (ATP) Assay kit (S0027), JC-1 Mitochondrial Membrane Potential Assay kit (C2006) and Reactive Oxygen Species Assay kit (S0033) were provided by Beyotime Institute of Biotechnology (Haimen, China).

Cell culture and viability assay. PC12 cells were maintained in Dulbecco's modified Eagle's medium (DMEM; Hyclone; GE Healthcare Life Sciences, Logan, Logan, UT, USA) supplemented with 10% fetal bovine serum (FBS; Gibco; Thermo Fisher Scientific, Inc., Waltham, MA, USA) and 1% Antibiotic Antimycotic solution consisting of 10,000 U penicillin and 10,000 U streptomycin. The cells were incubated at 37˚C in humidified atmosphere of 5% CO_2 and always used at 70-80% confluence.

The viability of PC12 cells was determined using a Cell Counting Kit (CCK-8; Dojindo Molecular Technologies, Inc., Shanghai, China). Cells were seeded into 96-well plates at a density of $1x10^5$/well. After 24 h culture, cells were treated with NaN_3 (0-80 mM) and incubated for 12, 24, 48 and 72 h to establish the cell injury model. Subsequently, 10 μl CCK-8 solution (Dojindo Molecular Technologies, Inc.) was added to each well and incubated for an additional 2 h under the standard conditions (37˚C and 5% CO_2). The absorbance at a wavelength of 450 nm was determined by ELx808 Absorbance Microplate Reader (BioTek Instruments, Inc., Winooski, VT, USA). The cell viability was calculated according to the mean optical density of 6 wells. The experiments were conducted in triplicate. The appropriate concentrations of NaN_3 for use in subsequent experiments were determined according the results of the cell viability assays.

Nuclear morphology of DAPI-stained PC12 cells. PC12 cells were exposed to 0, 10, 20 and 40 mM NaN_3 for 24 h. In order to distinguish programmed cell death from non-apoptotic cell death, nuclei were stained with 10 μg/ml DAPI (C1005; Beyotime Institute of Biotechnology). Briefly, cells were washed twice with PBS and then fixed with 4% paraformaldehyde at room temperature for 30 min. Subsequent to three washes, fixed cells were stained with DAPI (1:5,000) for 5 min and then washed with PBS. Fluorescence images were acquired with a Leica DMI fluorescence microscope (magnification, x400).

Measurement of apoptotic rate. An Annexin V-FITC/PI Apoptosis Detection kit (Beyotime Institute of Biotechnology) was used to determine apoptosis of cells according to the manufacturer's instructions. Experiments were repeated in triplicate and were performed as follows: The apoptotic rates of control PC12 cells (0 mM NaN_3) and PC12 cells exposed to 10, 20 and 40 mM NaN_3 for 24 h was measured by flow cytometry (FC500; Beckman Coulter, Inc., Brea, CA, USA). Statistical analyses were conducted with SPSS statistical software v.13.0 (SPSS, Inc., Chicago, IL, USA).

Measurement of mitochondrial membrane potential ($\Delta\Psi m$). ΔΨm is a significant parameter of mitochondrial function. It was assessed using staining with JC-1, a fluorescent probe. Experiments were repeated in triplicate, and were performed as follows: Control PC12 cells were treated with 0 mM NaN_3; and experimental PC12 cells were exposed to 10, 20 and 40 mM NaN_3 for 24 h. Subsequently, according to the manufacturer's protocol (C2006; Mitochondrial Membrane Potential Assay kit; Beyotime Institute of Biotechnology, Haimen, China), cells were incubated with the medium containing JC-1 (1X) at 37˚C for 20 min, the cells were washed three times with wash buffer and collected with fresh medium without serum. Concomitantly, the positive control was treated with carbonyl cyanide 3-chlorophenylhydrazone (CCCP), an inhibitor, (10 μM) at 37˚C for 20 min. Then, the red/green fluorescence was determined by FCM (FC500; Beckman Coulter, Inc.). The ratios of red fluorescence intensity over green fluorescence intensity represented the levels of $\Delta\Psi m$.

Measurement of reactive oxygen species (ROS) production. ROS in PC12 cells was assessed using a Reactive Oxygen Species Assay kit (S0033; Beyotime Institute of Biotechnology, Haimen, China). Intracellular ROS generation was assessed by means of 2',7'-dichlorofluorescein diacetate (DCFH-DA), a fluorescent probe. Intracellular ROS oxidizes DCFH-DA, yielding the fluorescent compound 2',7'-dichlorofluorescein (DCF), and DCF fluorescence intensity is considered to be parallel to the amount of formed ROS, according to the instructions of the ROS assay kit. Experiments were repeated in triplicate and performed as follows: Positive control were treated with specific concentration of Rosup (50 mg/ml); control PC12 cells were

Table I. NaN_3 suppresses the growth of PC12 cells (n=6).

NaN_3 concentration (mmol/l)	Time interval, h (% viability)			
	12	24	48	72
0	100	100	100	100
5	98.21±7.84	39.33±3.99	33.69±3.34	27.29±12.99
10	95.94±1.47	34.86±7.98	26.06±3.22	19.7±9.91
20	90.57±2.87	24.89±3.33	12.99±2.83	7.52±4.65
40	87.21±0.46	16.89±0.73	4.40±1.36	2.19±1.49
80	74.78±2.97	7.35±2.55	1.37±0.73	0.65±1.44

Data are presented as the mean ± standard deviation. NaN_3, sodium azide.

treated with 0 mM NaN_3; and experimental PC12 cells were exposed to 10, 20 and 40 mM NaN_3 for 24 h. In addition, PC12 cells were treated with DCFH-DA (10 mM) dissolved in serum-free DMEM (1:1,000) for 20 min at 37˚C and then washed three times with serum-free DMEM. The positive control was treated with Rosup, to induce ROS production. The ROS production was determined by FCM (FC500; Beckman Coulter, Inc.). The Mean fluorescence intensities (MFI) represented the levels of ROS.

Measurement of cellular ATP content in PC12 cells. Experiments were repeated in triplicate and performed as follows: Control PC12 cells were treated with 0 mM NaN_3; and experimental PC12 cells were exposed to NaN_3 at different concentrations (10, 20 and 40 mM) for 24 h. Subsequently, the cellular ATP content was determined using a Firefly Luciferase ATP Assay kit (Beyotime Institute of Biotechnology) according to the protocol of the manufacturer.

Western blot analysis. PC12 cells were exposed to 0, 10, 20 and 40 mM NaN_3 for 24 h, lysed in radioimmunoprecipitation assay lysis buffer (Beyotime Institute of Biotechnology) containing a protease inhibitor and centrifuged at 13,362 x g for 10 min at 4˚C in order to collect the supernatants. Subsequently, the protein concentrations were determined using BCA kit (Pierce; Thermo Fisher Scientific, Inc.). Equal amounts of proteins (90 μg) were subjected to 10 and 12% SDS-PAGE, and then transferred onto polyvinylidene fluoride membranes (0.45 μm) using a Semidry Electro-transfer Unit (Bio-Rad Laboratories, Inc., Hercules, CA, USA). Following blocking with 5% bovine serum albumin in TBS containing 0.1% Tween-20 (TBST) for 2 h at room temperature, the membranes were incubated with primary antibodies against Pgc-1α (Abcam, Cambridge, MA, USA; 1:500), Nrf-2 (Abcam; 1:500), Cox IV (Abcam; 1:1,000), Tfam (Abcam; 1:1,000), procaspase-3 (Abcam; 1:500), Nrf-1 (Cell Signaling Technology, Inc., Danvers, MA, USA, 1:500), pan-calcineurin A (CaN; Cell Signaling Technology Inc.; 1:1,000), phosphorylated (p)-CaMKII (Cell Signaling Technology; 1:1,000), p-p38 MAPK (Cell Signaling Technology, Inc.; 1:1,000), p-extracellular signal-regulated kinase (Erk)1/2 (Cell Signaling Technology, Inc.; 1:1,000), B-cell lymphoma-2 (Bcl-2)-associated X protein (Bax; Santa Cruz Biotechnology, Inc., Dallas, TX, USA; 1:200), Bcl-2 (Santa Cruz Biotechnology, Inc.; 1:200) and cytochrome c (Santa Cruz Biotechnology, Inc.; 1:200) at 4˚C overnight. The membranes were then washed with TBST and incubated with horse-radish peroxidase (HRP)-conjugated secondary antibodies (rabbit; cat. no. A0208; 1:1,000; or mouse; cat. no. A0216; 1;1,000; both Beyotime Institute of Biotechnology) for 1 h at room temperature. Immunoreactive bands were visualized by the enhanced chemiluminescence system (Clinx Science Instruments Co., Ltd., Shanghai, China) and quantitatively analyzed with Image J version 1.32 J (National Institutes of Health, Bethesda, MD USA), and β-actin was selected as the loading control.

Statistical analysis. All statistical analyses were conducted with SPSS statistical software v.13.0 (SPSS, Inc., Chicago, IL, USA). Data are expressed as the mean ± standard deviation standard error of the mean. The statistical significance of differences between groups was determined by one-way analysis of variance followed by Bonferroni post-hoc tests. $P<0.05$ was considered to indicate a statistically significant difference. Each experiment was repeated least three times.

Results

NaN_3 inhibits the growth of PC12 cells. The effect of NaN_3 exposure on the proliferation of PC12 cells was assessed by CCK-8 assay. Cells were challenged with different concentrations (0-80 mM) of NaN_3 for 12-72 h. Table I and Fig. 1A-D indicate that the cell viability was decreased by NaN_3 in a concentration-dependent manner. Almost 100% of the cells died following exposure to 80 mM NaN_3 for 72 h, indicating that NaN_3 markedly induced cell death, and the cytotoxicity of NaN_3 was detected in a dose- and time-dependent manner. Exposure to NaN_3 at a concentration of 20 mM for 24 h caused marked cell death in the PC12 cells (50%). Therefore, the cells cultured for 24 h were used for subsequent experiments.

Cell morphology. In DAPI staining, the morphological changes of PC12 cells were observed by fluorescence microscopy following exposure to different concentrations of NaN_3. The fragmentation of cell nuclei exposed to NaN_3 for 24 h was observed, and cell nuclei shrinkage and chromatin condensation were increased slightly with the concentration of NaN_3 in

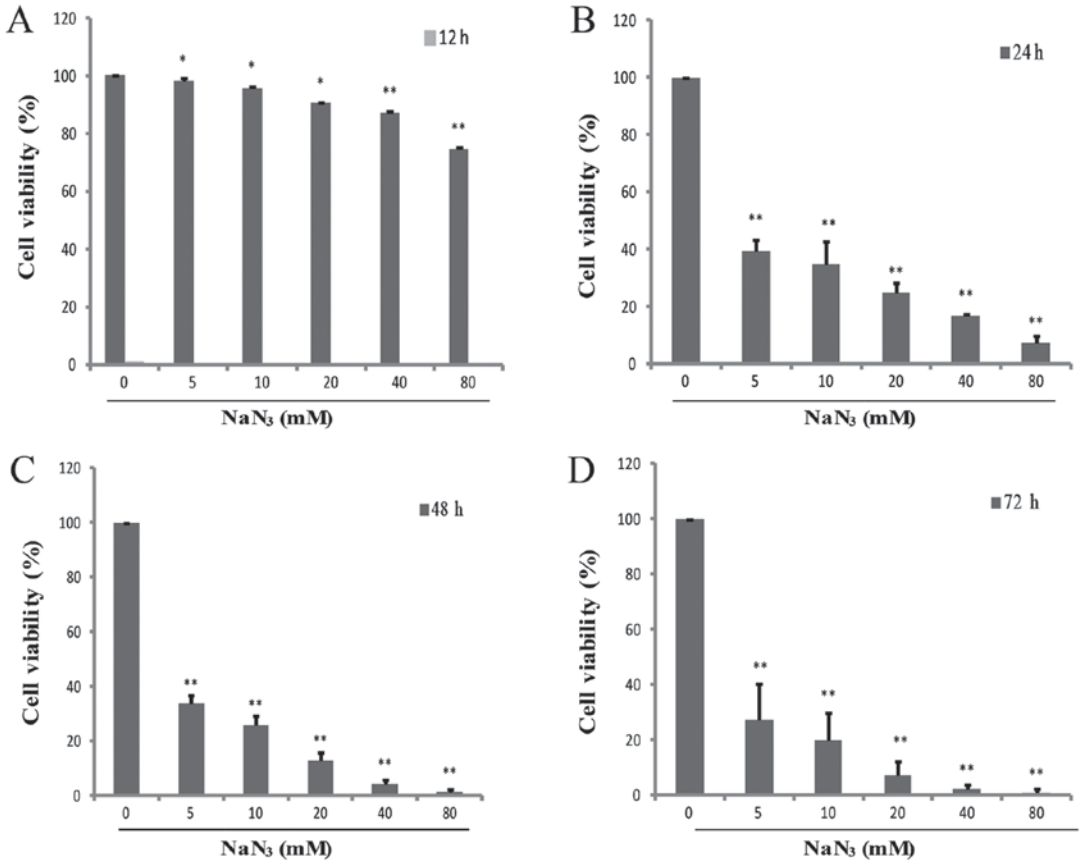

Figure 1. NaN_3 suppresses cell viability in cultured PC12 cells. Following exposure to 0, 5, 10, 20, 40 and 80 mM NaN_3 for 24 h, the survival rate was decreased to 100, 39.33±3.99, 34.86±7.98, 24.89±3.33, 16.89±0.73 and 7.35±2.55%, respectively. The cytotoxicity in PC12 cells was detected at (A) 12, (B) 24, (C) 48 and (D) 72 h by CCK-8 assay. *P<0.05 and **P<0.01 vs. the control group. NaN_3, sodium azide.

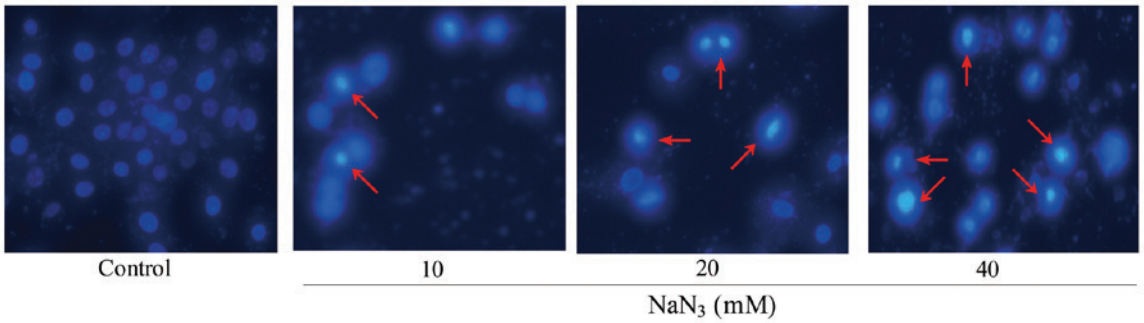

Figure 2. Effects of NaN_3 on nuclear morphology in PC12 cells. Morphological changes of PC12 cells were revealed by DAPI staining and visualized under fluorescence microscopy upon exposure to different concentrations of NaN_3 (0, 10, 20 and 40 mM). Arrows indicates NaN_3-induced nuclear shrinkage and chromatin condensation. Magnification, x200. NaN_3, sodium azide.

PC12 cells as compared to the control. In these cells, apoptotic cells were smaller and brighter compared with normal cells. Chromatin condensation and nuclear fragmentation were also observed, whereas blue nuclei of viable cells were identified in the control group. In addition, the number of apoptotic cells and the intensity of green fluorescence were increased in cells exposed to NaN_3 (Fig. 2).

Apoptotic rate determination by Annexin V-FITC staining. Dead cells or late apoptotic cells that have lost cell membrane integrity may be stained by propidium iodide. Due to the loss of this cell membrane integrity, Annexin V-FITC may enter into the cytoplasm and combine with the phosphatidylserine inside of the cell membrane, exhibiting green fluorescence in dead cells. Fig. 3 demonstrates that the numbers of apoptotic cells were 5.03, 8.02, 43.77 and 78.67% (P<0.05) in the PC12 cells following exposure to NaN_3 at different concentrations (0, 10, 20 and 40 mM) for 24 h, respectively. These results additionally confirmed that NaN_3 induced cell apoptosis in a dose-dependent manner.

Changes in mitochondrial membrane potential (ΔΨm). Mitochondria are generally considered key regulatory organelles involved in cell viability. Therefore, ΔΨm was used as the

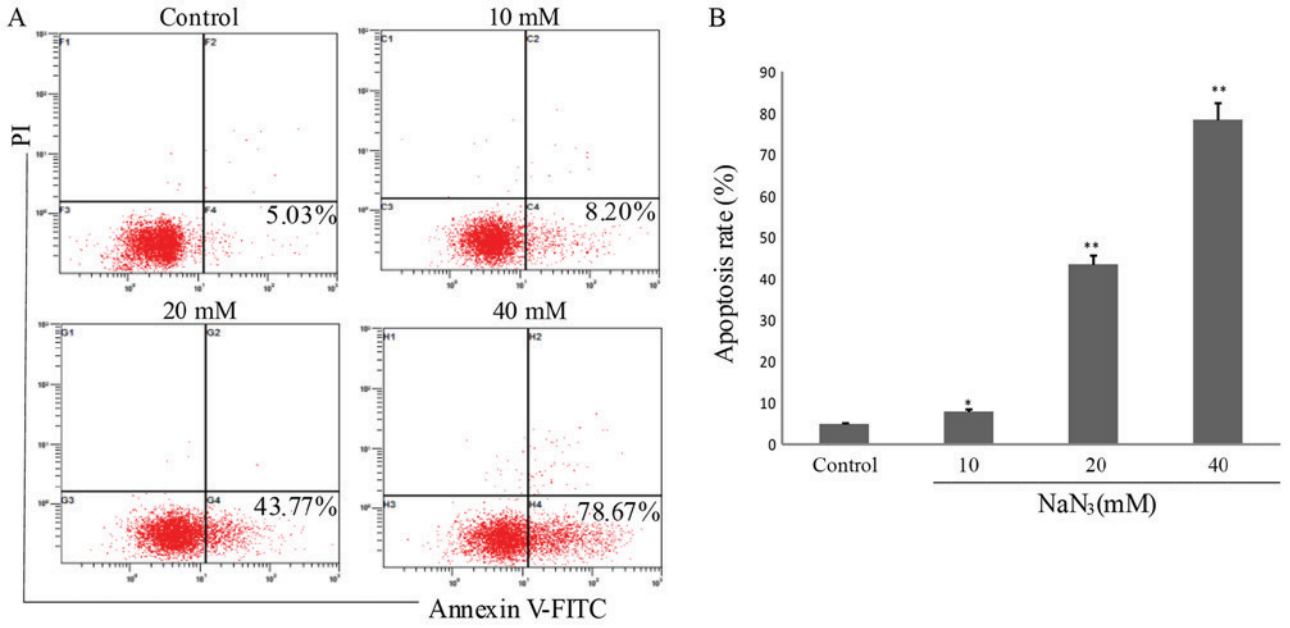

Figure 3. Detection of cell apoptosis in PC12 cells by Annexin V-FITC/PI staining. Cells were exposed to different concentrations of NaN_3 (0, 10, 20 and 40 mM) for 24 h. (A) PC12 cells were stained with Annexin V-FITC/PI and analyzed by flow cytometry. (B) Quantitative analysis of NaN_3-induced apoptosis. Proportions of apoptotic cells are presented as mean ± standard deviation (n=3). *P<0.05 and **P<0.01 vs. the control group. FITC, fluorescein isothiocyanate; PI, propidium iodide; NaN_3, sodium azide.

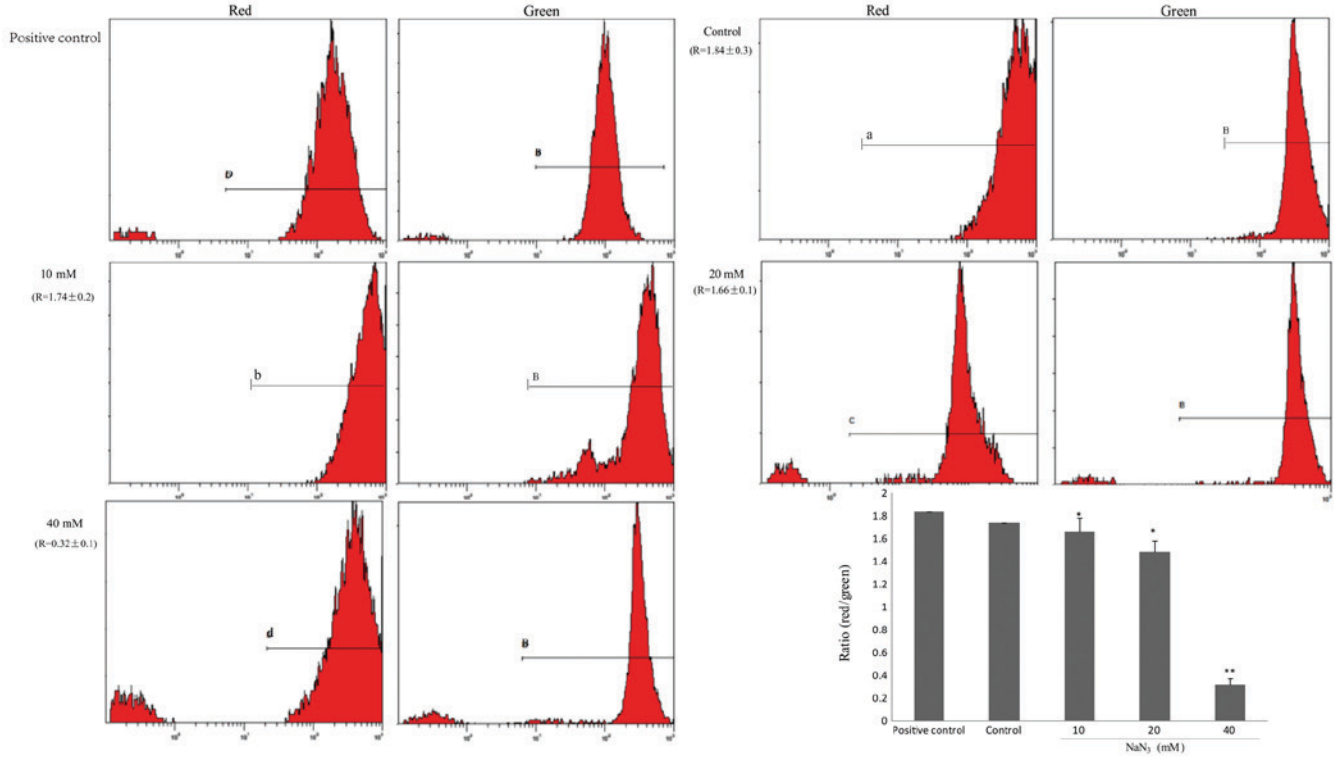

Figure 4. NaN_3 exposure decreases the ΔΨm. Cells were exposed to different concentrations of NaN_3 (0, 10, 20 and 40 mM) for 24 h. ΔΨm was detected by flow cytometry. The ratio of red/green fluorescence was calculated to assess the relative ΔΨm. Data were expressed as mean ± standard deviation (n=3). *P<0.05 and **P<0.01 vs. the control group. NaN_3, sodium azide; ΔΨm, mitochondrial membrane potential.

indicator of mitochondrial function. PC12 cells were stained with JC-1, a cationic dye that exhibits potential-dependent accumulation in mitochondria. Red fluorescence (J-aggregates), representing active mitochondria with stable membrane potential, was observed in a small number of cells exposed to increasing concentrations of NaN_3. By contrast, green fluorescence (J-monomer), representing apoptotic mitochondria with damaged ΔΨm, was observed in a number of cells. The ratio of red and green fluorescence gradually decreased in the control group (Fig. 4).

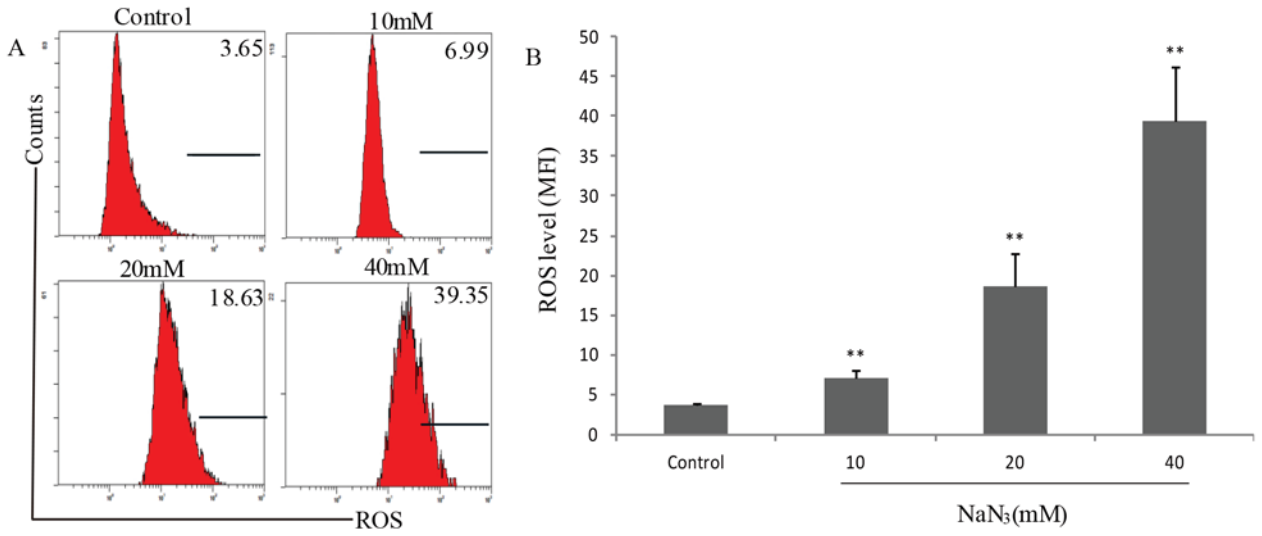

Figure 5. Effects of NaN_3 on ROS level in PC12 cells. Cells were exposed to different concentrations of NaN_3 (0, 10, 20 and 40 mM) for 24 h. (A) The fluorescence intensity was measured by flow cytometry. (B) Quantitative analysis of the ROS level. NaN_3 exposure significantly increased the production of mitochondrial ROS compared with the control group. Data were expressed as the means ± standard deviation (n=3). **P<0.01 vs. the control group. NaN_3, sodium azide; ROS, reactive oxygen species; MFI, mean fluorescence intensity.

NaN_3-induced accumulation of mitochondrial ROS. It is well known that mitochondria are the primary source of cellular ROS, and ROS serve an important role in activation of apoptotic signaling. Therefore, the role of ROS in NaN_3-induced PC12 cell death was additionally investigated. Fig. 5 indicates that the fluorescence intensities in control cells and cells exposed to NaN_3 at various concentrations (0, 10, 20 and 40 mM) for 24 h were 3.65, 6.99, 18.63 and 39.35, respectively, indicating that NaN_3 exposure significantly increased the production of mitochondrial ROS compared with the control group (P<0.05). These results suggested that NaN_3-induced apoptosis improved the production of intracellular ROS.

NaN_3 downregulates the mitochondrial energy production of cellular ATP. To evaluate the ATP content in PC12 cells exposed to NaN_3, the relative luminescence unit (RLU) was quantitatively determined by a luminometer. Fig. 6 indicates that NaN_3 inhibited mitochondrial ATP production and gradually decreased the cellular ATP level (P<0.05).

Expression levels of Pgc-1α and apoptosis-associated proteins in PC12 cells. The Pgc-1α expression at the protein level was significantly decreased following NaN_3 exposure compared with the control (P<0.05). In addition, Nrf-1, Tfam, p-Erk1/2, Nrf-2 and Cox IV are well-known downstream targets of Pgc-1α dynamics in various cell types (8). The present study identified that NaN_3 exposure significantly inhibited Pgc-1α dynamics in a dose-dependent manner (P<0.01; Fig. 7A).

In addition, NaN_3 exposure upregulated the expression levels of Bax and cytochrome c, while it downregulated the expression levels of Bcl-2 and procaspase-3 (P<0.05). The ratio of Bax/Bcl-2 was also significantly increased compared with the control group (P<0.05; Fig. 7B).

The protein expression levels of other important members, including CaN, CaMKII, p-CaMKII, p38 MAPK and p-p38 MAPK, were also assessed. The results indicated that NaN_3 increased the expression of CaN and the phosphorylation of CaMKII and p38 MAPK compared with the control group, while the expression levels of total CaMKII and p38 MAPK were not changed. In addition, the ratios of p-CaMKII/CaMKII and p-p38/p38 MAPK in the NaN_3 group were significantly increased compared with those in the control group (P<0.01; Fig. 7C).

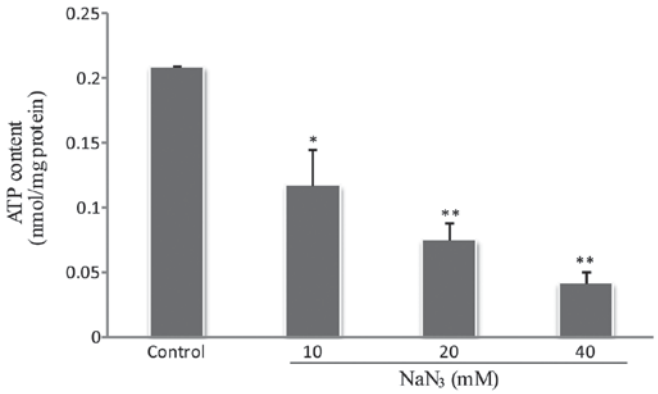

Figure 6. NaN_3 inhibits the production of intracellular ATP. Cells were exposed to NaN_3 for 24 h, and the ATP level in PC12 cells was measured with an enhanced ATP assay kit. Data were expressed as mean ± standard deviation (n=3). *P<0.05 and **P<0.01 vs. the control group. NaN_3, sodium azide; ATP, adenosine 5'-triphosphate.

Discussion

To determine whether NaN_3 inhibited the proliferation of PC12 cells, the number of treated cells in the logarithmic phase was compared with the number of non-treated control cells. Cell growth was inhibited by ~75% after 24 h of exposure to 20 mM NaN_3. Therefore, this concentration was used for subsequent experiments. Apoptosis involves changes

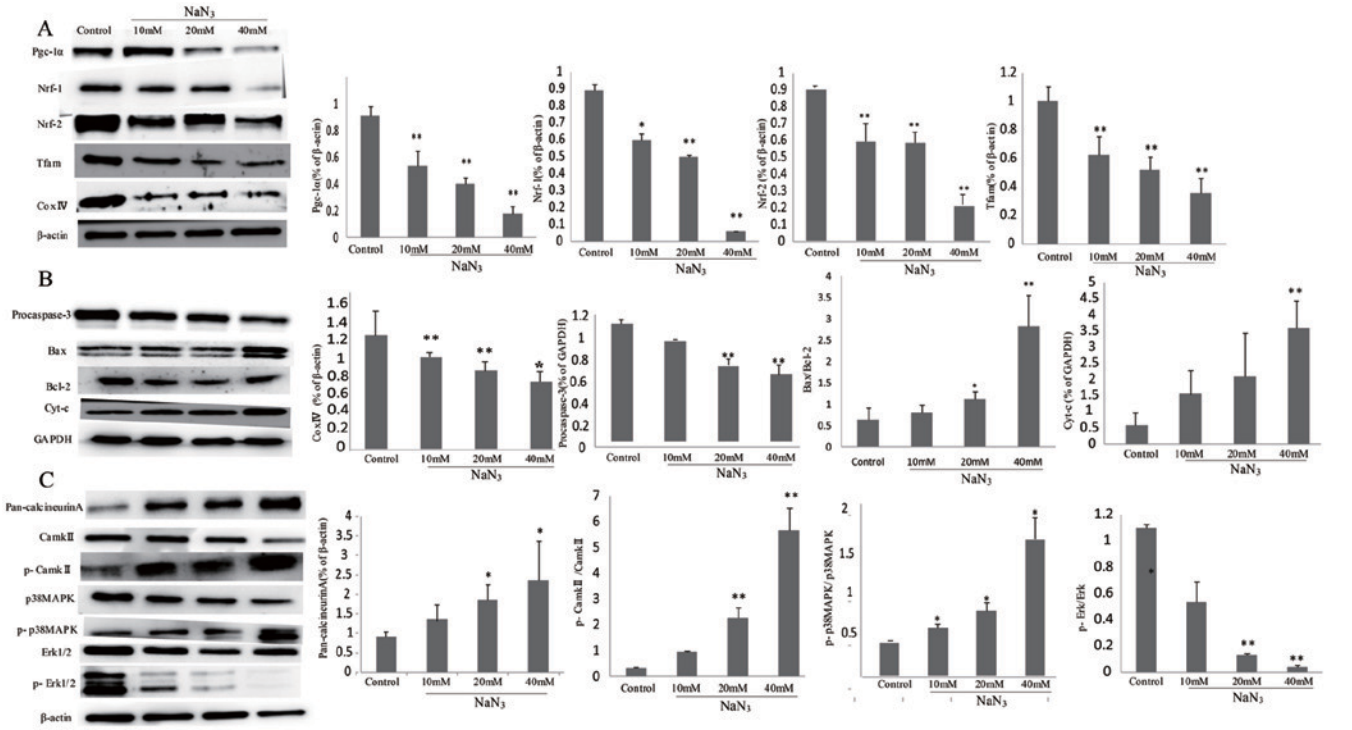

Figure 7. NaN_3 induces mitochondria-mediated apoptosis through the expression of Pgc-1α-associated proteins in PC12 cells. (A) Expression levels of Pgc-1α, Nrf-1, Nrf-2, Tfam and Cox IV detected by western blot analysis. (B) Expression levels of procaspase-3, Bax, Bcl-2 and cyt-c detected by western blot analysis. (C) Expression levels of pan-calcineurin A, CaMKII, p-CaMKII, p38 MAPK, p-p38 MAPK, Erk1/2 and p-Erk1/2 detected by western blot analysis. β-actin and GAPDH were used as the internal control. Band intensity ratios for each group are presented as mean ± standard deviation (n=3). *P<0.05 and **P<0.01 vs. the control group. Pgc-1α, peroxisome proliferator-activated receptor γ co-activator 1-α; Nrf-1/2, nuclear respiratory factor-1/2; Tfam. Mitochondrial transcription factor A; Cox IV, complex IV; Bcl-2, B-cell lymphoma 2; Bax, Bcl-2-associated X protein; cyt-c, cytochrome c; CaMKII, Ca^{2+}/calmodulin-dependent protein kinase II; p, phosphorylated; p38 MAPK, p38 mitogen-activated protein kinase; Erk1/2, extracellular signal-regulated kinase 1/2.

in cellular morphology, including membrane blebbing, cell shrinkage, chromatin condensation, nuclear fragmentation and DNA fragmentation (9). To additionally analyze nuclear morphology of apoptosis and apoptotic rate, cells were challenged with 0, 10, 20 and 40 mM NaN_3 for 24 h. Following treatment, cells were then stained with DAPI and Annexin V-FITC/PI, and the distribution of the nuclei was analyzed. The results confirmed that NaN_3 exposure induced apoptosis in PC12 cells in a concentration-dependent manner.

Mitochondria are involved in numerous metabolic functions, including maintenance of intracellular pH and production of ROS, which promote and regulate cell apoptosis (10). The hallmarks of cell apoptosis are preceded by mitochondrial alterations, including a loss of ΔΨm, a decrease in energy production (ATP) and an increase in permeability of the mitochondrial membrane. Previous studies have suggested that ROS trigger damage to the mitochondrial respiratory chain and induce the loss of ΔΨm, which are the factors that mediate or amplify the neuronal dysfunction during the course of the neurodegeneration, consequently leading to the development of neurodegenerative diseases (11,12). NaN_3 is known to drive degeneration and excitotoxicity by increasing the permeability potential of the mitochondrial membrane through lipid peroxidation (13-15), and NaN_3 exerts its primary toxic action by inhibiting the function of cytochrome oxidase in the mitochondrial electron transport chain and preventing the ATP production (4). In the present study, FCM was used to identify ΔΨm and ROS production in PC12 cells. In addition, the ATP synthesis in mitochondria was examined following exposure to various concentrations of NaN_3. The disruption of the plasma membrane, the increase of mitochondrial ROS production and the decrease in cellular ATP content observed suggested that NaN_3 exposure induced the apoptosis in PC12 cells.

Mitochondrial cell death may be activated by multiple stimuli, including the developmental program, DNA damage, endoplasmic reticulum stress, growth factor and nutrient deprivation, viral infection and oxidative stress (16). As a member of the ever-growing family of nuclear co-regulators, Pgc-1α may activate a large set of genes and regulate the expression levels of genes involved in energy metabolism in response to signaling pathways that mediate thermogenesis, gluconeogenesis, muscle fiber type switching and mitochondrial biogenesis (17). These co-regulators exist and function in large multi-protein complexes, in which rather than binding to DNA, they regulate Nrf-1/2 and Tfam and modulate their transcriptional potency by promoting the subsequent biochemical interactions required for induction or repression of gene transcription (8). In addition, Nrf-1/2 also indirectly controls the expression of mitochondrial DNA-encoded genes by potently inducing the nuclear-encoded Tfam A, B1 and B2 (Tfam, Tfb1m and Tfb2m, respectively), which are the regulators of the transcription and replication of the mitochondrial genome (18). Previous studies have demonstrated that NaN_3 is an inhibitor of the mitochondrial respiratory

chain complex IV, which is frequently affected in primary mitochondrial disorders (19,20). In the present study, the expression of Pgc-1α signal cascade, including Pgc-1α family proteins (Pgc-1α, Nrf-1, Nrf-2 and Tfam) and Cox IV, was first examined in PC12 cells to verify whether the signaling events were involved in NaN_3-induced apoptosis. The results suggested that the NaN_3-induced apoptosis was associated with the expression levels of Pgc-1α family proteins and Cox IV in mitochondria-mediated signaling pathway. When the concentrations of NaN_3 were increased, the expression levels of these proteins were significantly decreased, indicating that they may be involved in the activation and development of apoptosis.

Conversely, complex IV may trigger apoptosis in primary cortical neurons, which is caspase3-dependent and associated with the release of cytochrome c (5). It is well known that mitochondria are key regulators of cell apoptosis. The Bcl-2 family proteins are the important initiators of the mitochondrial apoptotic pathway. This family includes the pro-apoptotic proteins Bax, Bcl-2 homologous antagonist/killer and Bcl-2-associated agonist of cell death and anti-apoptotic proteins Bcl-2 and Bcl-extra large (Bcl-xL). In healthy cells, Bax is an inactive cytosolic protein, but it is translocated into the mitochondria during apoptosis. It exerts its pro-apoptotic effects by forming a pore in the mitochondrial outer membrane, through which cytochrome c is released into the cytoplasm, leading to the activation of caspase 3 (21). The anti-apoptotic proteins Bcl-2 and Bcl-xL suppress the function of Bax by maintaining integrity of mitochondrial membrane, which prevents the release of cytochrome c and the activation of caspase 3 (22). In the present study, NaN_3 increased the levels of pro-apoptotic Bax and cytochrome c and decreased levels of anti-apoptotic Bcl-2 and procaspase-3, indicating that NaN_3 initiated mitochondrial apoptosis signaling in PC12 cells.

In addition, the expression levels of Pgc-1α co-activators are highly inducible at the transcriptional level via a variety of upstream signaling pathways. For example, the expression of Pgc-1α is induced by exercise and cold exposure under the control of stress signaling via cellular Ca^{2+} and cyclic adenosine 5'-monophosphate (cAMP) signaling (23). The transcription of Pgc-1α may be affected by CaMK, calcineurin, β-adrenergic receptor/cAMP and p38 MAPK (24-26). In addition, p38 MAPK belonging to the MAPK family serves a pivotal function in cell proliferation, differentiation, transformation and apoptosis, since the activation of apoptosis may induce Pgc-1α via direct phosphorylation (27). In the present study, the expression levels of proteins in Ca^{2+} signaling pathways (pan-calcineurin A and p-CaMKII/CaMKII) and p38 MAPK pathway (p-p38MAPK/p38 MAPK and p-Erk1/2) were examined to investigate the effects of NaN_3 on intracellular Ca^{2+} homeostasis and p38 MAPK. The data indicated that the protein levels of pan-calcineurin A, and the p-CaMKII/CaMKII and p-p38 MAPK/p38 MAPK ratios were increased and p-Erk1/2 level was decreased in the NaN_3-treated group, suggesting that NaN_3 triggered the apoptosis of PC12 cells in a dose-dependent manner, and such an activation was associated with the Ca^{2+} and p38 MAPK pathways. Taken together, these experimental results confirmed that NaN_3 may induce the apoptosis of PC12 cells by activating Ca^{2+} and p38 MAPK pathways. To the best of our knowledge, the present study revealed for the first time that NaN_3 induced mitochondria-mediated apoptosis in PC12 cells through Pgc-1α-associated signaling pathways, including Ca^{2+}/p-CaMKII and p38 MAPK.

In summary, the present study demonstrated that NaN_3 may induce the apoptosis of PC12 cells. In order to elucidate the underlying toxic mechanism of NaN_3 exposure, the expression levels of a series of pro-apoptotic proteins (Bax and cytochrome c) and anti-apoptotic proteins (Bcl-2, procaspase-3, p-p38 MAPK, p-CaMKII and Pgc-1α) were examined. The results confirmed that pro-apoptotic proteins exerted pro-apoptotic effects on PC12 cells via activation and phosphorylation of CaMKII and p38 MAPK, which stimulated the activation of Pgc-1α and procaspase-3 in PC12 cells. The data provide a basis for subsequent studies investigating NaN_3 mechanisms of action at the molecular level. Future studies may include the addition of protective agents, for example mitochondrial division inhibitor 1, a derivative of quinazolinone that is a newly-identified mitochondrial division inhibitor, prior to NaN_3 treatment, in order to investigate the neuroprotective effects of the protective agent in attenuating NaN_3-induced apoptosis in PC12 cells, and to additionally elucidate the underlying mechanism.

Acknowledgements

Not applicable.

Funding

The present study was financially supported by the grants from the National Natural Science Foundation of China (grant no. 81571848) and the Priority Academic Program Development of Jiangsu Higher Education Institutions.

Availability of data and materials

The datasets used or analyzed during the present study are available from the corresponding author on reasonable request.

Authors' contributions

YZ and SZ conceived and designed the study. YZ, JH, HX, TG and YW acquired the data. YZ, JH and HX analyzed and interpreted the data, and drafted the manuscript. All authors critically revised the manuscript, and read and approved the final version of the manuscript.

Ethics approval and consent to participate

Not applicable.

Patient consent for publication

Not applicable.

Competing interests

The authors declare that they have no competing interests.

References

1. Herbold M, Schmitt G, Aderjan R and Pedal I: Fatal sodium azide poisoning in a hospital: A preventable accident. Arch Kriminol 196: 143-148, 1995 (In German).
2. Marquet P, Clément S, Lotfi H, Dreyfuss MF, Debord J, Dumont D and Lachâtre G: Analytical findings in a suicide involving sodium azide. J Anal Toxicol 20: 134-138, 1996.
3. Chang S and Lamm SH: Human health effects of sodium azide exposure: A literature review and analysis. Int J Toxicol 22: 175-186, 2003.
4. Leary SC, Hills BC, Lyons CN, Carison CG, Michaud D, Kraft CS, Ko K, Glerum DM and Moyes CD: Chronic treatment with azide in situ leads to an irreversible loss of cytochrome c oxidase activity via holoenzyme dissociation. J Biol Chem 277: 11321-11328, 2002.
5. Grammatopoulos TN, Morris K, Bachar C, Moore S, Andres R and Weyhenmeyer JA: AngiotensinII attenuates chemical hypoxia-induced caspase-3 activation in primary cortical neuronal cultures. Brain Res Bull 62: 297-303, 2004.
6. Scarpulla RC: Metabolic control of mitochondrial biogenesis through the PGC-1 family regulatory network. Biochim Biophys Acta 1813: 1269-1278, 2011.
7. Qian G, Guo JB and Li L: The role of Pgc-1α and mitochondrial regulation in cardiovascular disease. Chinese Pharmacol Bull 29: 1-5, 2013.
8. Jones AW, Yao Z, Vicencio JM, Karkucinska-Wieckowska A and Szabadkai G: PGC-1 family coactivators and cell fate: Roles in cancer, neurodegeneration, cardiovascular disease and retrograde mitochondria-nucleus signaling. Mitochondrion 12: 86-99, 2012.
9. Kerr JFR, Winterford CM and Harmon BV: Apoptosis: Its significance in cancer and cancer therapy. Cancer 73: 2013-2026, 1994.
10. Chan DC: Mitochondria: Dynamic organelles in disease, ageing and development. Cell 125: 1241-1252, 2006.
11. Islam MT: Oxidative stress and mitochondrial dysfunctionlinked neurodegenerative disorders. Neurol Res 39: 73-82, 2017.
12. Chaturvedi RK and Flint BM: Mitochondrial diseases of the brain. Free Radic Biol Med 63: 1-29, 2013.
13. Van Laar VS, Roy N, Liu A, Raiprohat S, Arnold B, Dukes AA, Holbein CD and Berman SB: Glutamate excitotoxicity in neurons triggers mitochondrial and endoplasmic reticulum accumulation of Parkin and in the presence of N-acetyl cysteine, mitophagy. Neurobiol Dis 74: 180-193, 2015.
14. Liu L, Peritore C, Ginsberg J, Shinh J, Arun S and Donmez G: Protective role of SIRT5 against motor deficit and dopaminergic degeneration in MPTP-induced mice model of Parkinson's disease. Behav Brain Res 281: 215-221, 2015.
15. Palomo GM and Manfredi G: Exploring new pathways of neurodegeneration in ALS: The role of mitochondria quality control. Brain Res 1607: 36-46, 2015.
16. Youle RJ and Strasser A: The BCL-2 protein family: Opposing activities that mediate cell death. Nat Rev Mol Cell Biol 9: 47-59, 2008.
17. Vercauteren K, Pasko RA, Gleyzer N, Marino VM and Scarpulla RC: PGC-1-related coactivator: Immediate early expression and characterization of a CREB/NRF-1 binding domain associated with cytochrome c promoter occupancy and respiratory growth. Mol Cell Biol 26: 7409-7419, 2006.
18. Scarpulla RC: Transcriptional paradigms in mammalian mitochondrial biogenesis and function. Physiol Rev 88: 611-638, 2008.
19. Betts J, Lightowlers RN and Turnbull DM: Neuropathological aspects of mitochondrial DNA disease. Neurochem Res 29: 505-511, 2004.
20. Tanji K, Kunimatsu T, Vu TH and Bonilla E: Neuropathological features of mitochondrial disorders. Semin Cell Dev Biol 12: 429-439, 2001.
21. Aluvila S, Mandal T, Hustedt E, Fajer P, Choe JY and Oh KJ: Organization of the mitochondrial apoptotic BAK pore: Oligomerization of the BAK homodimers. J Biol Chem 289: 2537-2551, 2014.
22. Yang E, Zha J, Jockel J, Boise LH, Thompson CB and Korsmeyer SJ: Bad, a heterodimeric partner for Bcl-XL and Bcl-2, displaces Bax and promotes cell death. Cell 80: 285-291, 1995.
23. Hock MB and Kralli A: Transcriptional control of mitochondrial biogenesis and function. Annu Rev Physiol 71: 177-203, 2009.
24. Handschin C, Rhee J, Lin J, Tarr PT and Spieglman BM: An autoregulatory loop controls peroxisome proliferator-activated receptor gamma coactivator 1alpha expression in muscle. Proc Natl Acad Sci USA 100: 7111-7116, 2003.
25. Schaeffer PJ, Wende AR, Magee CJ, Neilson JR, Leone TC, Chen F and Kelly DP: Calcineurin and calcium/calmodulin-dependent protein kinase activate distinct metabolic gene regulatory programs in cardiac muscle. J Biol Chem 279: 593-603, 2004.
26. Rohas LM, St-Pierre J, Uldry M, Jäger S, Handschin S and Spiegelman BM: A fundamental system of cellular energy homeostasis regulated by PGC-1 alpha. Proc Natl Acad Sci USA 104: 7933-7938, 2007.
27. Puigserver P, Rhee J, Lin J, Wu Z, Yoon JC, Zhang CY, Krauss S, Mootha VK, Lowell BB and Spiegelman BM: Cytokine stimulation of energy expenditure through p38 MAP kinase activation of PPARgamma coactivator-1. Mol Cell 8: 971-982, 2001.